Calhoun: The NPS Institutional Archive

DSpace Repository

Theses and Dissertations | 1. Thesis and Dissertation Collection, all items

1957

A study of the wake at supersonic air flow of elliptical body - flat disk combination using hydraulic analogy to compressible air flow

Geer, Jon Roger

Monterey, California. Naval Postgraduate School

http://hdl.handle.net/10945/24865

Downloaded from NPS Archive: Calhoun

http://www.nps.edu/library

Calhoun is the Naval Postgraduate School's public access digital repository for research materials and institutional publications created by the NPS community. Calhoun is named for Professor of Mathematics Guy K. Calhoun, NPS's first appointed -- and published -- scholarly author.

Dudley Knox Library / Naval Postgraduate School
411 Dyer Road / 1 University Circle
Monterey, California USA 93943

A STUDY OF THE WAKE AT SUPERSONIC AIR FLOW OF AN ELLIPTICAL BODY - FLAT DISK COMBINATION USING HYDRAULIC ANALOGY TO COMPRESSIBLE AIR FLOW

A Thesis Submitted to the Graduate Faculty
of the
University of Minnesota

by

Jon Roger Geer
Lieutenant, United States Navy

In Partial Fulfillment of the Requirements
for the Degree of
Master of Science in Aeronautical Engineering

June, 1957

Theatre
G2577

TABLE OF CONTENTS

35766

A STUDY OF THE WAKE AT SUPERSONIC AIR FLOW OF AN ELLIPTICAL BODY - FLAT DISK COMBINATION USING HYDRAULIC ANALOGY TO COMPRESSIBLE AIR FLOW

SUMMARY

The problem investigated herein is the Mach number recovery in the wake of an elliptical cylinder in a supersonic flow whose free stream Mach number is approximately 2.00. Using the hydraulic analogy to simulate conditions in compressible gas flow, Mach number recovery is determined by measurement of the distances between the detached shock waves and a flat disk model towed at various distances behind the elliptical cylinder model.

Comparisons are made between the theoretical forms and locations of detached shock waves ahead of blunt bodies in air and the observed forms and locations of detached hydraulic jumps ahead of blunt bodies in water.

Condensed hydraulic analogy and detached shock wave theories are included in the appendices.

As a result of this investigation, the following conclusions are made:

a. A water channel provides a very inexpensive method for demonstrating two-dimensional wave characteristics in compressible gas flow. Within the limitation of the hydraulic analogy, quantitative data of the wave formation can be obtained by carefully controlling the water depth and velocity.

b. The hydraulic analogy is valid for use in the study of leading edge shock waves caused by flow deflections approaching the shock wave detachment angle for a double-wedge.

c. The detached shock wave theory very closely predicts the forms of detached shock waves ahead of blunt bodies.

d. Mach number recovery in the wake of an elliptical cylinder at a free stream Mach number of approximately 2.00 is 90 percent complete at a downstream distance of approximately 2.4 model widths. Recovery is 95 percent complete at a downstream distance of approximately 3.4 model widths.

e. At downstream distances equal to or greater than seven times the model width, the flow between the trailing edge shock waves of an elliptical cylinder is uniform.

f. Until confirmed by experimental evidence obtained in a supersonic wind tunnel, the quantitative data in d above must be viewed only as a guide for use in planning wind tunnel experiments.

A STUDY OF THE WAKE AT SUPERSONIC AIR FLOW OF AN ELLIPTICAL BODY - FLAT DISK COMBINATION USING HYDRAULIC ANALOGY TO COMPRESSIBLE AIR FLOW

INTRODUCTION

This investigation was conducted for the purpose of determining the Mach number in the wake of an elliptical cylinder at downstream distances up to ten times the width of the cylinder and the observation of wave formations caused by various models. A free stream Mach number of approximately 2.00 was maintained during all test runs.

The hydraulic analogy to compressible gas flow has been demonstrated by Preiswerk[1]* and others. The simulation of shock waves in air by hydraulic jumps in water is the basis upon which this investigation was conducted. The form and the location of the detached shock waves produced by a flat disk in the wake of the elliptical cylinder provide the quantitative data for this report.

This experiment was conducted at the University of Minnesota, Minneapolis, Minnesota, during the school year 1956-1957.

It is desired here to express thanks to some of those whose assistance made this experiment possible; namely: to Professor John D. Akerman and Dr. Helmut G. Heinrich for their inspiration

* Numbers in parenthesis refer to references listed at the end of this report.

and many pertinent suggestions; to Mike Schonberg and Miles Mock for providing the necessary hardware; to Arvid Grikis for his assistance with the photographs and for reproducing the report; and to Stanley Markham and John Kallevig for the myriad jobs undertaken in the conduct of the investigation. Finally, to my wife, Marty, is extended my most sincere thanks for her uncomplaining endurance of three years of virtual solitude during the current "shore duty" tour.

TABLE OF SYMBOLS

a	speed of sound in a gas
β	cotangent of the Mach wave angle ($\sqrt{M^2 - 1}$)
cp	specific heat at constant pressure
c_v	specific heat at constant volume
γ	adiabatic gas constant, c_p/c_v
d	water depth
η	angle between sonic line and normal to free-stream direction
g	acceleration due to gravity
h	enthalpy or total heat content
λ	angle of streamline relative to x-axis
λ_d	wedge half-angle for which shock becomes detached
M	Mach number, stream values unless otherwise indicated (V/a for gas; $V/\sqrt{gd}$ for water)
μ	Mach wave angle ($\sin^{-1} \frac{1}{M}$)
p	pressure
ρ	Mass density
σ	isentropic contraction ratio from free stream to sonic velocity
T	absolute temperature of gas
V	velocity
u,v,	components of velocity in x-direction and y-direction, respectively
x,y,z	rectangular coordinate axes

SUBSCRIPTS

c	centroid of stream tube passing sonic line
o	value at stagnation (V = 0)
∞	value in undisturbed stream
S	sonic point of detached shock
SB	sonic point on body
s	conditions along sonic line
w	conditions in the wake of the elliptical cylinder model
x	partial derivative with respect to x (for example $\phi_x = \frac{\partial \phi}{\partial x}$; $\phi_{xx} = \frac{\partial^2 \phi}{\partial x^2}$)
y	partial derivative with respect to y

EQUIPMENT

Three models were used during this investigation, a photograph of which is included as Fig. 1. They are:

a. Double-wedge - constructed of pine lumber, 6.00 inches in length, having a half-angle of 20 degrees, waterproofed with boiled linseed oil and varnished to provide a smooth surface. The height of this model is approximately 1¼ inches.

b. Elliptical cylinder - constructed of pine lumber, 2.00 inches in length, 1.00 inch in width, approximately 1¼ inches in height, treated in the same manner as the double-wedge.

c. Flat disk - constructed of brass sheet stock 0.040 inch thickness, 1.00 inch wide and approximately one inch in height. A thin brass rod is soldered to this model to facilitate its being mounted onto the model tow carriage.

The models may be attached to tubular arms which extend out perpendicularly from model carriages mounted on an extruded aluminum monorail. This monorail is suspended approximately eight inches above the plate glass floor of the water basin used in this experiment. A photograph of the model set up is shown in Fig. 2.

The model carriage towing system is composed of a power and velocity control unit for the tow, and a closed circuit phosphorus-bronze stranded wire towline. The power and control unit is a 115 volt A. C. variable speed, reversible motor producing up to five inch-pounds of torque with an electronic speed adjustment. This unit is shown in Fig. 3.

The water basin used in this experiment is L-shaped, is four feet wide and has a maximum length of twelve feet. The plate

glass floor of the basin may be leveled by adjusting the height of the supporting legs. A complete description of the design of this basin is found in Ref. 2.

In order that the model speed could be measured accurately, a timing mechanism was constructed, consisting of a thin, formed copper contact, mounted on the forward model carriage, which is held by spring action against two thin brass rails inserted in grooves in a wooden beam mounted alongside the model carriage monorail. One of the brass rails is 38.8 inches in length, is mounted opposite the test section and serves as the timer strip, while the other rail extends over the entire length of the wooden beam. In order that the copper contact brush may smoothly traverse the entire length of the water basin, plexiglass strips are placed in the grooves on either side of the timer brass strip. A photograph of the timer mechanism is shown in Fig. 4. Each brass rail is connected by wiring to a modified Brush Oscillograph Recorder control unit (Fig. 5) in such a way that when the copper contact brush closes the circuit between the two brass rails, a 60-cycle signal is introduced to the oscillograph. When the model carriage has passed the test section and the copper contact brush has broken contact with the timer rail, this signal is abruptly interrupted. Paper tape is fed from the oscillograph recorder at the rate of 125 millimeters per second. Since the model speed is low (of the order of 1.6 feet per second), this timing device is quite accurate.

Since the speed of propagation of gravity waves in liquids is dependent upon the depth of the liquid (see Appendix A), it is

necessary to measure the depth of the liquid accurately. For this purpose a device was constructed, consisting of a micrometer mounted in a framework of aluminum sheets and wooden blocks, connected by wiring to an ohmmeter containing a small battery. A photograph of this device is included as Fig. 6. Tap water used in the water basin contains a sufficient amount of ionized minerals to be a good electrical conductor. One electrical lead is connected to the micrometer head and the other lead is placed in the water. When the micrometer shaft contacts the surface of the water, the ohmmeter needle is deflected. With this device, water depth can be measured with 0.001-inch accuracy. Caution must be exercised, however, in insuring that the micrometer shaft is perfectly dry and free of foreign matter in order that premature contact with the surface of the water is avoided.

With the use of the timer mechanism and the water depth measuring device, it is possible to compute the test section Mach number with accuracy to the second decimal place.

Photographs were made with a studio type camera mounted vertically on a tripod supported above the test section by a wooden frame, the camera lens being approximately four feet above the water line. Exposure times for all test run photographs were of 1/50 second duration. Lighting was provided by an electronic flash unit, the duration of the flash being 1/500 second. For the test runs, aperture openings of f16 and f22 were used. Eastman Super-Panchro, Type B, 4" X 5" sheet film was used to make all photographs.

Several photographic lighting arrangements were tried. It

was found that for the observation of the detached shock waves ahead of the models, the most desirable lighting arrangement is obtained when the electronic flash is placed slightly above the camera, aimed at the surface of the water slightly upstream of the models. The light reflected from the disturbed surface of the water provides a very good high-contrast photograph. A black velvet cloth was supported beneath the glass floor of the water basin to provide a dark background for the photographs. A view of the entire experimental set up is included as Fig. 7.

PROCEDURE

In what follows, a general knowledge of the theory of the hydraulic analogy to two-dimensional compressible air flow[1] is assumed. A summary of this theory is included as Appendix A. Appendix B contains a summary of an approximate method for predicting form and location of detached shock waves ahead of plane bodies[3].

Since Laitone[4] has analyzed the theory governing the propagation of surface water waves to show that an analogy with the two-dimensional flow of a perfect gas exists only if the water depth is approximately one-fourth inch, water depths in this experiment were maintained as near to 0.250 inch as practicable.

It is also known that the hydraulic analogy to compressible air flow becomes less valid at high Mach numbers. It was, therefore, decided to use a rather low supersonic Mach number for these test runs. Mach number 2.00 was arbitrarily chosen.

The following series of test runs were made:

a. Double-wedge alone

b. Elliptical cylinder alone

c. Flat disk alone

d. Flat disk placed directly in the wake of the elliptical cylinder at distances varying in one-inch increments from one inch to ten inches behind the trailing edge of the elliptical cylinder.

The bottom surface of each model was in sliding contact with the water basin floor at all times during each run.

The general procedure in making all the test runs was as follows:

a. Check and align model(s) to insure that the model(s) had no angle of attack.

b. Adjust depth of water to be as near 0.250 inch as practicable.

c. Using the timing device, make dummy runs, adjusting the motor control unit to provide model speed as near desired simulated Mach number 2.00 as practicable.

d. Check camera focus, using a printed card floating on the surface of the water as a focus target.

e. Again check and record the depth of the water.

f. Make test run, taking the photograph as the model(s) pass through the test section.

g. Record photographic data and test run Mach number.

Due to low relative humidity in the room containing the water basin, measurement of water depth had to be made very shortly before making each test run in order that the correct Mach number could be computed.

RESULTS AND DISCUSSION

The results of this investigation are contained in Table I and in Figs. 8 through 26. Fig. 8 is an overlay, depicting the theoretical shock wave pattern associated with a 20-degree half-angle double-wedge model in air. In Fig. 9, the actual shock wave produced by the double-wedge model in water is shown. The theoretical detached shock wave pattern ahead of the elliptical cylinder are shown in an overlay in Fig. 10. Fig. 11 shows the actual shock wave pattern associated with the elliptical cylinder. Fig. 12 is another overlay, showing the form and location of the theoretical detached shock wave ahead of the flat disk. Fig. 13 shows the actual shock wave associated with the flat disk. Based on the results of comparisons made in Figs. 12 and 13, a modified detached shock wave location theory for the flat disk model is plotted in Fig. 14.

In Figs. 15 through 20 and Figs. 22 through 25, shock wave patterns associated with the combination of the elliptical cylinder and the flat disk models are shown. Model separation distances in one-inch increments from one to ten inches downstream of the trailing edge of the elliptical cylinder model are shown. The theoretical detached shock wave ahead of the flat disk model is shown as an overlay in Fig. 21.

Mach number recovery in the wake of the elliptical cylinder is tabulated in Table I and plotted versus downstream distance in Fig. 26.

It is desired to establish the validity of comparing the form of hydraulic jumps in water caused by large flow deflection with shock waves produced under similar conditions in air. A double-

wedge model, upon which is impinged an attached leading edge shock wave, is ideal for making such comparisons. Theoretical shock wave angles for double-wedges in air flow are easily computed from Ref. 6. The wedge half-angle required for shock wave detachment in air at $M_\infty = 2.00$ is approximately 23 degrees. Therefore, a model whose half-angle is 20 degrees provides insurance that the shock wave will be attached even though the flow has been deflected through a significantly large angle. It is pertinent here to note that the leading edge shock wave remains straight only until it encounters the Mach waves caused by flow expansion around the model at its maximum width. For the model used in this experiment, this interaction takes place (at $M_\infty = 2.00$) approximately three inches in the downstream direction from the leading edge of the model.

A comparison of the theoretical and measured shock wave angles associated with the double-wedge model are shown in the unnumbered table below.

	Theoretical shock wave angle ($\gamma = 1.4$)	Measured shock wave angle
Leading edge shock	53.4°	54.4°
Trailing edge shock	20.4°	17.5°

It may be seen that the observed leading edge shock wave angle is in quite close agreement with the compressible gas shock wave theory. The discrepancy between theoretical and measured trailing edge shock wave angles is significant (approximately 15 percent). This discrepancy may be partially explained by the fact that the hydraulic analogy becomes less valid for flow deflections at higher Mach numbers. The theoretical Mach number on the rear face of the double-

wedge model is 2.74.

From the foregoing, it may be deduced that the hydraulic analogy is applicable, with certain reservations noted below, for the study of shock wave formations caused by large flow deflections.

In Figs. 10 and 11, comparison is made between the forms and locations of theoretical and observed detached shock waves ahead of the elliptical cylinder model. The dimension y_{SB} (see Appendix B) for an elliptical body is determined by the shock wave detachment angle, which is dependent upon the adiabatic constant γ. Therefore, theoretical shock wave forms and locations for both air ($\gamma = 1.40$) and the analogous gas ($\gamma = 2.00$) are shown. It is seen immediately that the locations of the theoretical shock waves are at considerable variance with the location of the observed shock wave. However, the forms of the theoretical shock wave for the analogous gas ($\gamma = 2.00$) and the observed shock wave are almost identical. It may be concluded that the theory developed by Moeckel[3] very closely predicts the form of a detached shock wave ahead of an elliptical cylinder model in water. However, as is also shown in Ref. 3, experimental data indicate that the theory places the location of the detached shock wave too close ahead of a blunt-nosed body in air.

Similar conclusions to those mentioned above may be drawn concerning the detached shock wave ahead of the flat disk model. In Fig. 12, a theoretical detached shock wave for air ($\gamma = 1.4$) is shown. The form of the theoretical shock wave in air was found to be very nearly the same as the observed form of the hydraulic jump in water. In view of the patterns shown in Fig. 10, it appears reasonable to assume that the form of the theoretical shock wave in

the analogous gas would be virtually identical to that of the observed pattern in water.

In order that the observed position of the detached shock wave ahead of the flat disk may be used to determine the Mach number ahead of the model it is necessary to modify the theory in the vicinity of $M_\infty = 2.00$. The distance L from the model to its detached shock wave (Fig. 13) at $M_\infty = 2.00$ is measured to be 0.85 inch. Since y_{SB} for the flat disk model is 0.50 inch, the dimension L/y_{SB} is 1.70. The dimension L/y_{SB} for $M_\infty = 2.00$ in accordance with Ref. 3 is 2.12. The ordinates of the theoretical curve of L/y_{SB} versus M_∞ from Ref. 3 are reduced by the ratio of 1.70 to 2.12 in Fig. 14. This reduction appears to be justified, in view of the fact that all measured data are in the vicinity of $M_\infty = 2.00$. Further, experimental data recorded in Ref. 3 indicate that it is to be expected that detached shock waves ahead of very blunt bodies will be farther removed than is predicted by the theory.

The location of the detached shock wave ahead of the flat disk in the wake of the elliptical cylinder is not perfectly clear in all photographs. Therefore, the measurement of the dimension L becomes largely a matter of judgment. In Figs. 17 through 20, the assumed locations of the foremost points of the detached shock waves are indicated.

The distance L from the flat disk model to its associated detached shock wave for each test run is tabulated in Table I. The value of L/y_{SB} is then used with Fig. 14 to determine the corresponding Mach number. To make the Mach number recovery presentation nondimensional, each measured Mach number is divided by M_∞. A plot

of M_w/M_∞ versus downstream distance from the elliptical cylinder model is made in Fig. 26, using the shock wave positions as positions of measured wake Mach numbers. Due to the rather large distances between the shock waves and the model, it is believed that the positions of the shock waves themselves more nearly define the positions of measured Mach numbers than do the positions of the model. It is noted here that for model separations of one and two inches Figs. 15 and 16), no characteristic detached shock wave appears ahead of the flat disk model. It must therefore be concluded that the flow immediately behind the trailing edge of the elliptical cylinder model is subsonic. This, of course, is to be expected in viscous flow.

It is seen in Fig. 26 that the wake Mach number recovery in the analogous gas is 90 percent complete at a downstream distance of approximately 2.4 model widths and is 95 percent complete at a downstream distance of approximately 3.4 model widths. Beyond that point, the wake Mach number recovery is quite gradual, approaching 100 percent recovery asymptotically.

The first downstream flat disk model position for which a complete, clearly defined detached shock wave is visible between the trailing edge shock waves of the elliptical model is shown in Fig. 22. Since it is desired to compare the form of the detached shock wave in this area with the theoretical shock wave, an overlay is included as Fig. 21. In Fig. 21, the theoretical detached shock wave for the flat disk in a free air stream corresponding to the computed wake Mach number is shown. This theoretical shock wave is corrected for location in accordance with the modified L/y_{SB} curve shown in

Fig. 14. It can be seen that, except for the deviation caused by interaction between the detached shock wave and the trailing edge shock waves of the elliptical cylinder, the observed form of the hydraulic jump agrees fairly well with the theory in a free air stream. In view of the comparison made between the shock waves in air ($\gamma = 1.4$) and the analogous gas ($\gamma = 2.0$) in Fig. 10, it is suspected that the theoretical detached shock wave for the analogous gas would be very nearly identical to the hydraulic jump observed in Fig. 22. A similar comparison also was made with Fig. 25, the results being the same. It may be concluded, therefore, that at downstream distances equal to or greater than seven times the model width, the flow between the trailing edge shock waves of the elliptical cylinder is uniform.

A search of the available literature fails to reveal a previous investigation of this nature in air. Therefore, the data provided by this experiment are not corroborated. In view of the foregoing, it must be concluded that until confirmed by investigators using two-dimensional models in a supersonic wind tunnel with a Reynolds number of approximately 22,500 based on the length of the elliptical cylinder model, the quantitative data shown herein must be viewed only as a convenient guide for use in planning wind tunnel experiments.

CONCLUSIONS

From the results of this investigation the following conclusions may be made.

a. A water channel provides a very inexpensive method for qualitatively demonstrating two-dimensional compressible gas flow phenomena. Within the limitations of the hydraulic analogy, quantitative data can be obtained by carefully controlling the water depth and velocity.

b. The hydraulic analogy is valid for use in the study of leading edge shock waves caused by large flow deflections.

c. The theory developed by Moeckel[3] very accurately predicts the forms of detached shock waves ahead of blunt bodies. However, as is also shown in Ref. 3, this investigation indicates that the theory places the locations of the detached shock waves too close ahead of blunt bodies.

d. Mach number recovery in the wake of an elliptical cylinder at $M_\infty = 2.00$ is 90 percent complete at a downstream distance of approximately 2.4 model widths. Recovery is 95 percent complete at a downstream distance of approximately 3.4 model widths.

e. At downstream distances equal to or greater than seven times the model width, the flow between the trailing edge shock waves of the elliptical cylinder is uniform.

f. Until confirmed by experimental evidence obtained in a supersonic wind tunnel, the quantitative data shown herein must be viewed only as a convenient guide for use in the planning of wind tunnel experiments.

REFERENCES

1. Preiswerk, E.: Applications of the Methods of Gas Dynamics to Water Flows with Free Surfaces. NACA TM 934, 1940

2. Lemeshewsky, A. A.: A Visual Investigation of the Interaction of Shock Waves from a Body in Curvilinear Diving Flight by Simulated Surface Waves on Water. University of Minnesota Thesis, 1955

3. Moeckel, W. E.: Approximate Method for Predicting Form and Location of Detached Shock Waves Ahead of Plane or Axially Symmetric Bodies. NACA TN 1921, 1949

4. Laitone, E. V.: A Study of Transonic Gas Dynamics by Hydraulic Analogy. Journal of the Aeronautical Sciences, Volume 19, Number 4, April, 1952

5. Orlin, W. J., N. J. Lindner and J. G. Bitterly: Application of the Analogy Between Water Flow With a Free Surface and Two-Dimensional Compressible Air Flow. NACA Report 875, 1946

6. Ames Research Staff: Equations, Tables, and Charts for Compressible Flow. NACA Report 1135, 1953

TABLE I

MACH NUMBER RECOVERY IN THE WAKE OF AN ELLIPTICAL CYLINDER

Model separation (inches)	M_∞	$\frac{L}{y_{SB}}$	M_w	$\frac{M_w}{M_\infty}$	Shock location from cylinder (inches)
1	2.00	(subsonic)	-	-	-
2	1.98	(subsonic)	-	-	-
3	2.06	2.19	1.72	0.835	1.905
4	2.00	1.89	1.88	0.940	3.055
5	1.95	1.90	1.87	0.959	4.050
6	2.03	1.77	1.95	0.960	5.115
7	2.06	1.72	1.99	0.966	6.140
8	2.00	1.81	1.92	0.960	7.095
9	2.03	1.72	1.99	0.981	8.140
10	2.02	1.81	1.92	0.951	9.095

FIG. 1
TEST MODELS

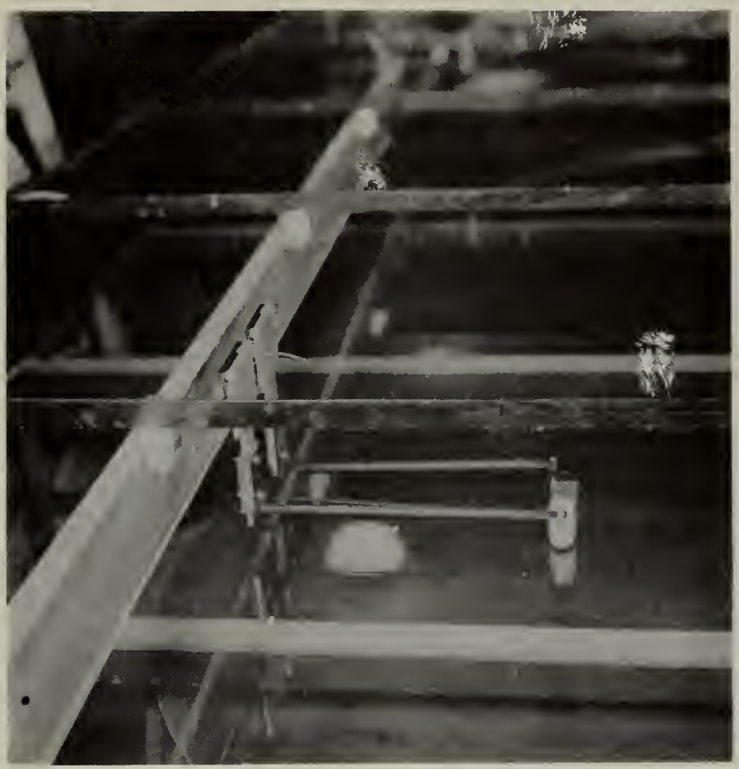

FIG. 2
MODEL TEST SET UP

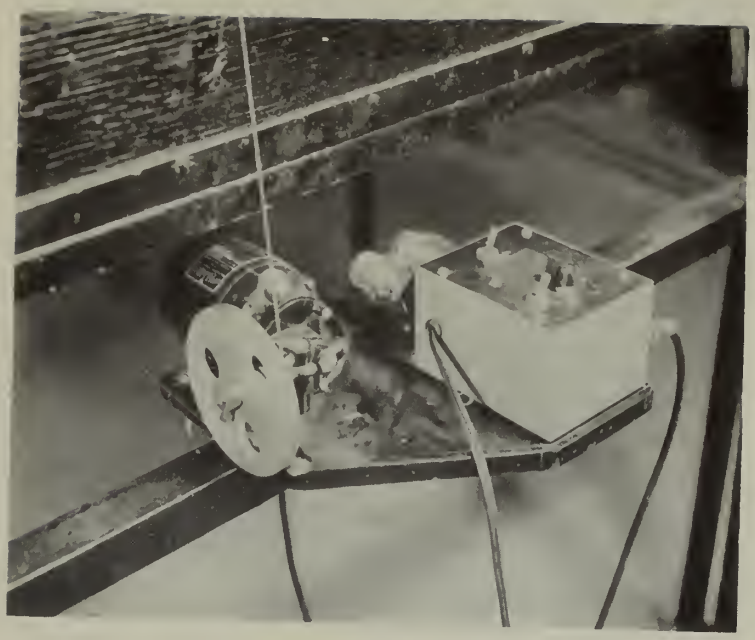

FIG. 3
TOW MOTOR AND CONTROL UNIT

FIG. 4
TIMER MECHANISM

FIG. 5
OSCILLOGRAPH RECORDER AND CONTROL UNIT

FIG. 6
WATER DEPTH MEASURING DEVICE

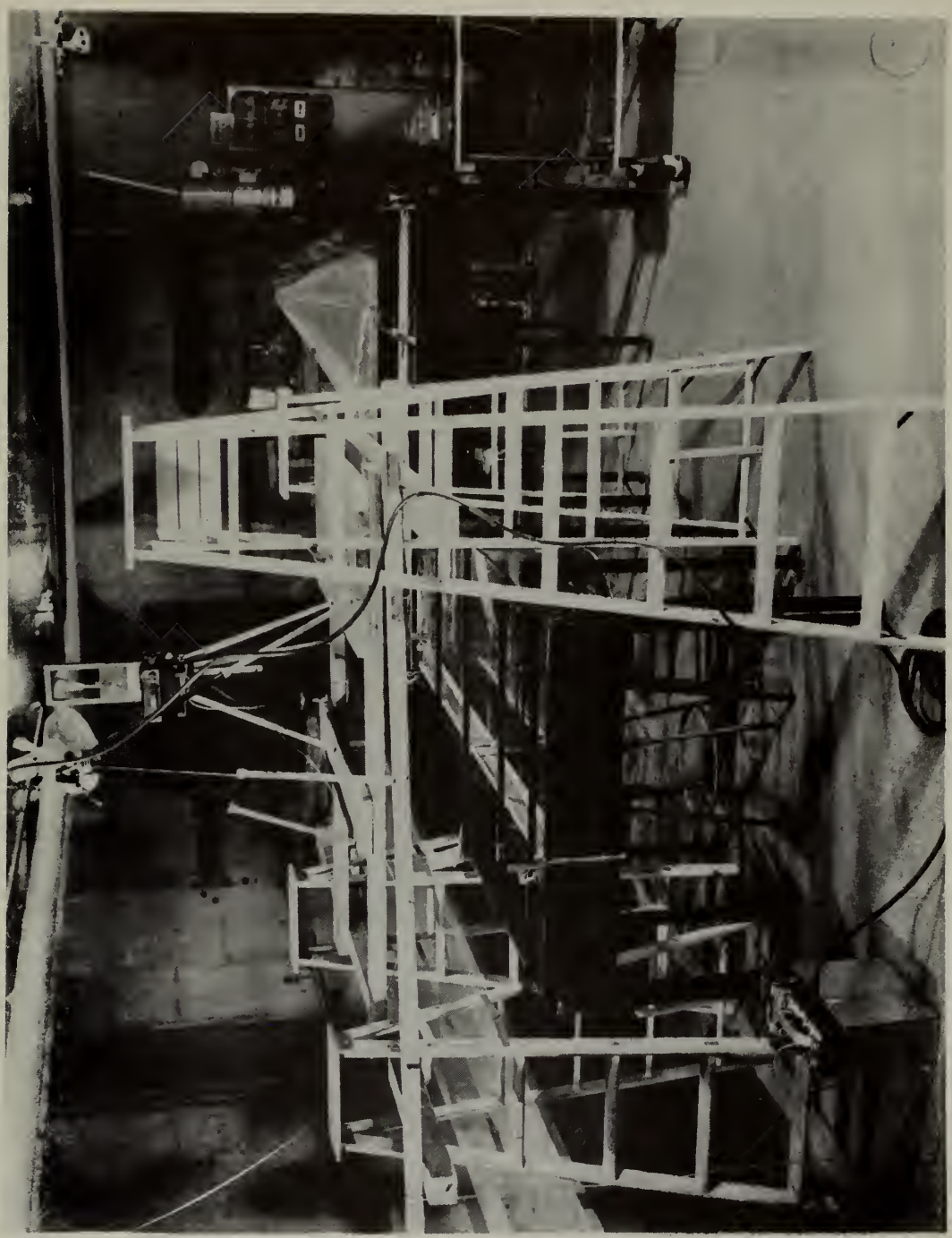

FIG. 7
PANORAMIC VIEW OF EXPERIMENTAL SET UP

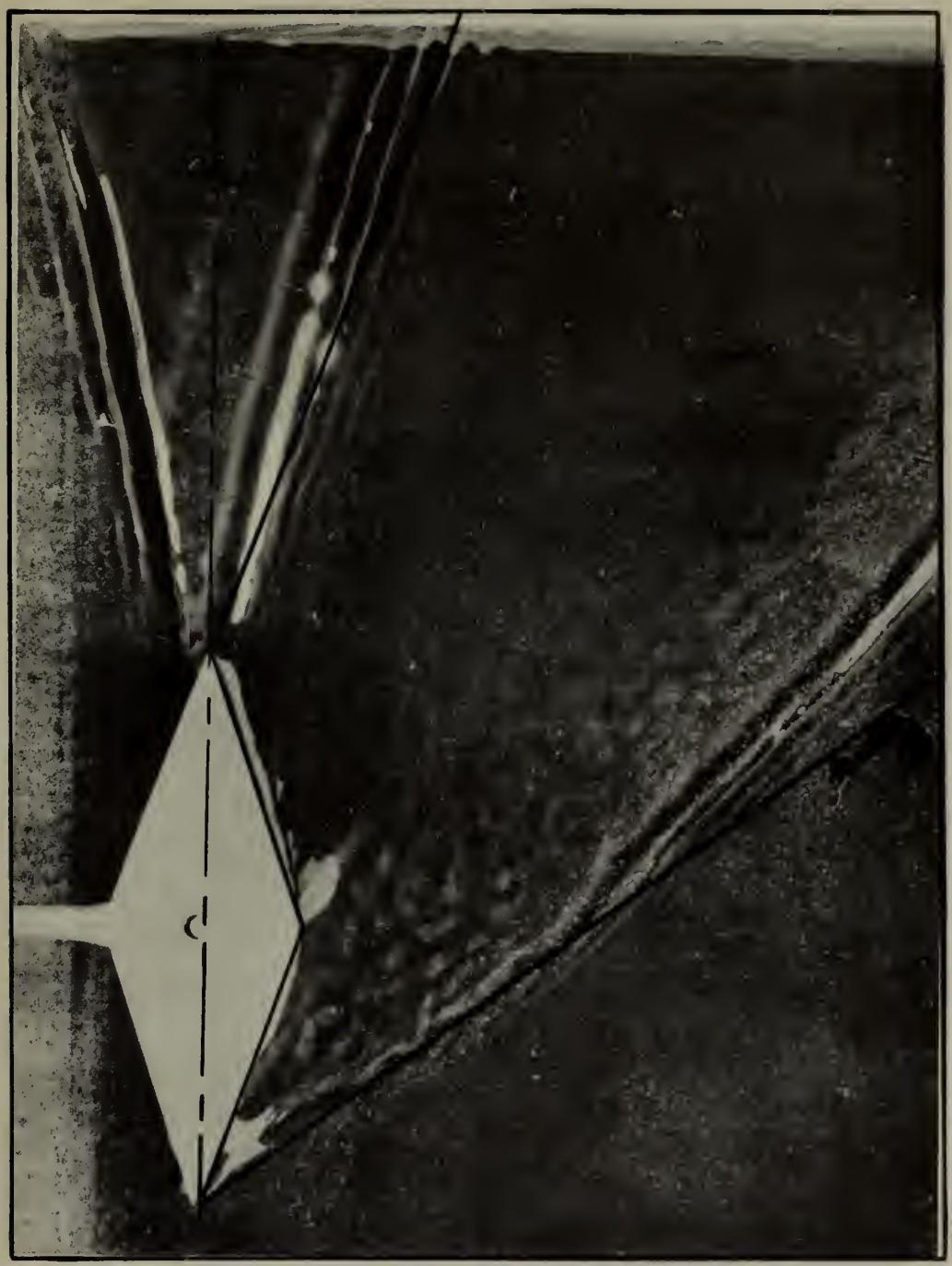

FIG. 9
DOUBLE-WEDGE (M_∞ = 2.00)

FIG. 8
THEORETICAL SHOCK WAVE PATTERN
FOR DOUBLE-WEDGE MODEL IN AIR
(OVERLAY FOR FIG. 9)

FIG. 11
ELLIPTICAL CYLINDER (M_∞ = 1.98)

FIG. 10
THEORETICAL DETACHED SHOCK WAVES
AHEAD OF ELLIPTICAL CYLINDER MODEL
(OVERLAY FOR FIG. 11)

FIG. 13
FLAT DISK ($M_\infty = 2.00$)

FIG. 12
THEORETICAL DETACHED SHOCK WAVE
AHEAD OF FLAT DISK MODEL
(OVERLAY FOR FIG. 13)

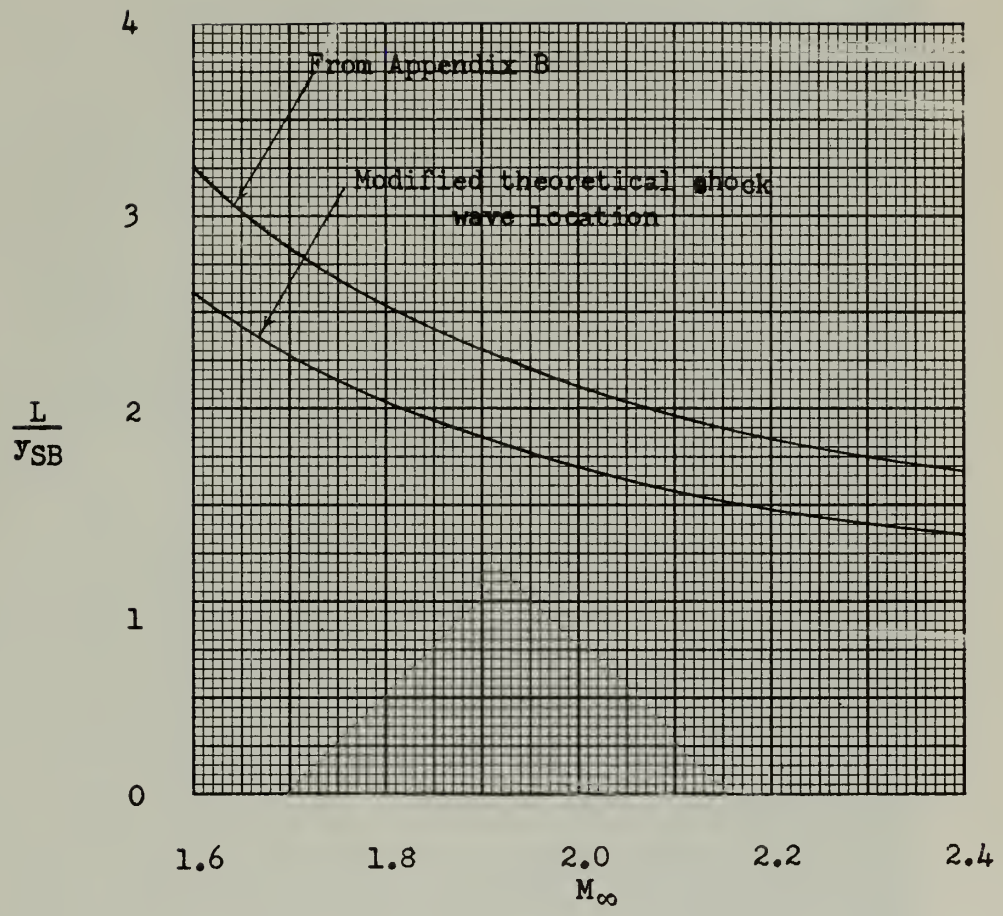

FIG. 14
MODIFIED THEORETICAL LOCATION OF
DETACHED SHOCK WAVE AHEAD OF FLAT
DISK MODEL IN THE VICINITY OF $M_\infty = 2.00$

FIG. 15
ELLIPTICAL CYLINDER - FLAT DISK COMBINATION
(1" SEPARATION - M_∞ = 2.00)

FIG. 16
ELLIPTICAL CYLINDER - FLAT DISK COMBINATION
(2" SEPARATION - $M_\infty = 1.98$)

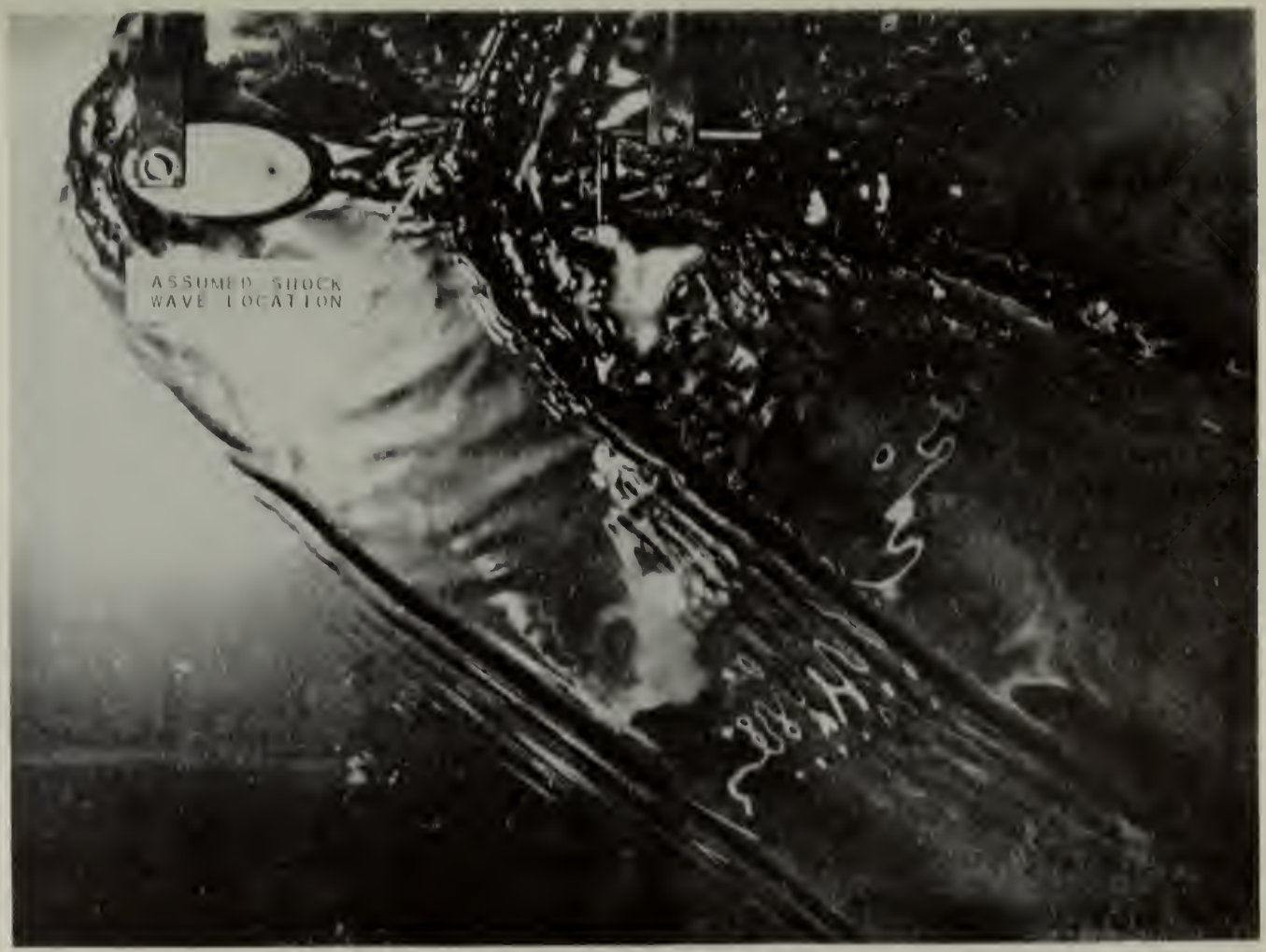

FIG. 17
ELLIPTICAL CYLINDER - FLAT DISK COMBINATION
(3" SEPARATION - M_∞ = 2.06)

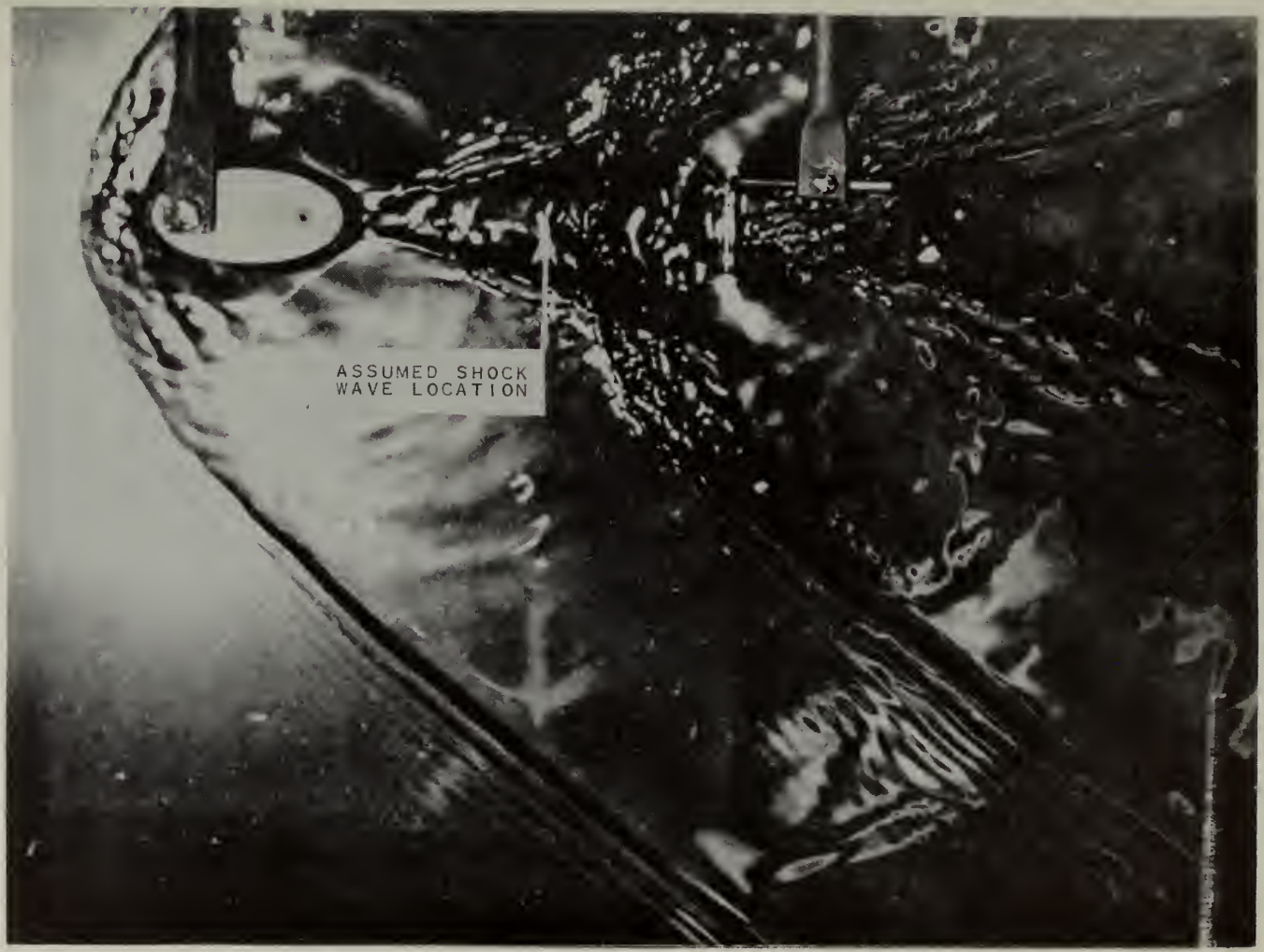

FIG. 18
ELLIPTICAL CYLINDER - FLAT DISK COMBINATION
(4" SEPARATION - $M_\infty \doteq 2.00$)

FIG. 19
ELLIPTICAL CYLINDER - FLAT DISK COMBINATION
(5" SEPARATION - M_∞ = 1.95)

FIG. 20
ELLIPTICAL CYLINDER - FLAT DISK COMBINATION
(6" SEPARATION - M_∞ = 2.03)

FIG. 22
ELLIPTICAL CYLINDER - FLAT DISK COMBINATION
(7" SEPARATION - $M_\infty = 2.06$)

FIG. 21
THEORETICAL SHOCK WAVE PATTERN CAUSED BY
FLAT DISK IN FREE STREAM AT $M_\infty = 1.99$
(OVERLAY FOR FIG. 22)

FIG. 23
ELLIPTICAL CYLINDER - FLAT DISK COMBINATION
(8" SEPARATION - M_∞ = 2.00)

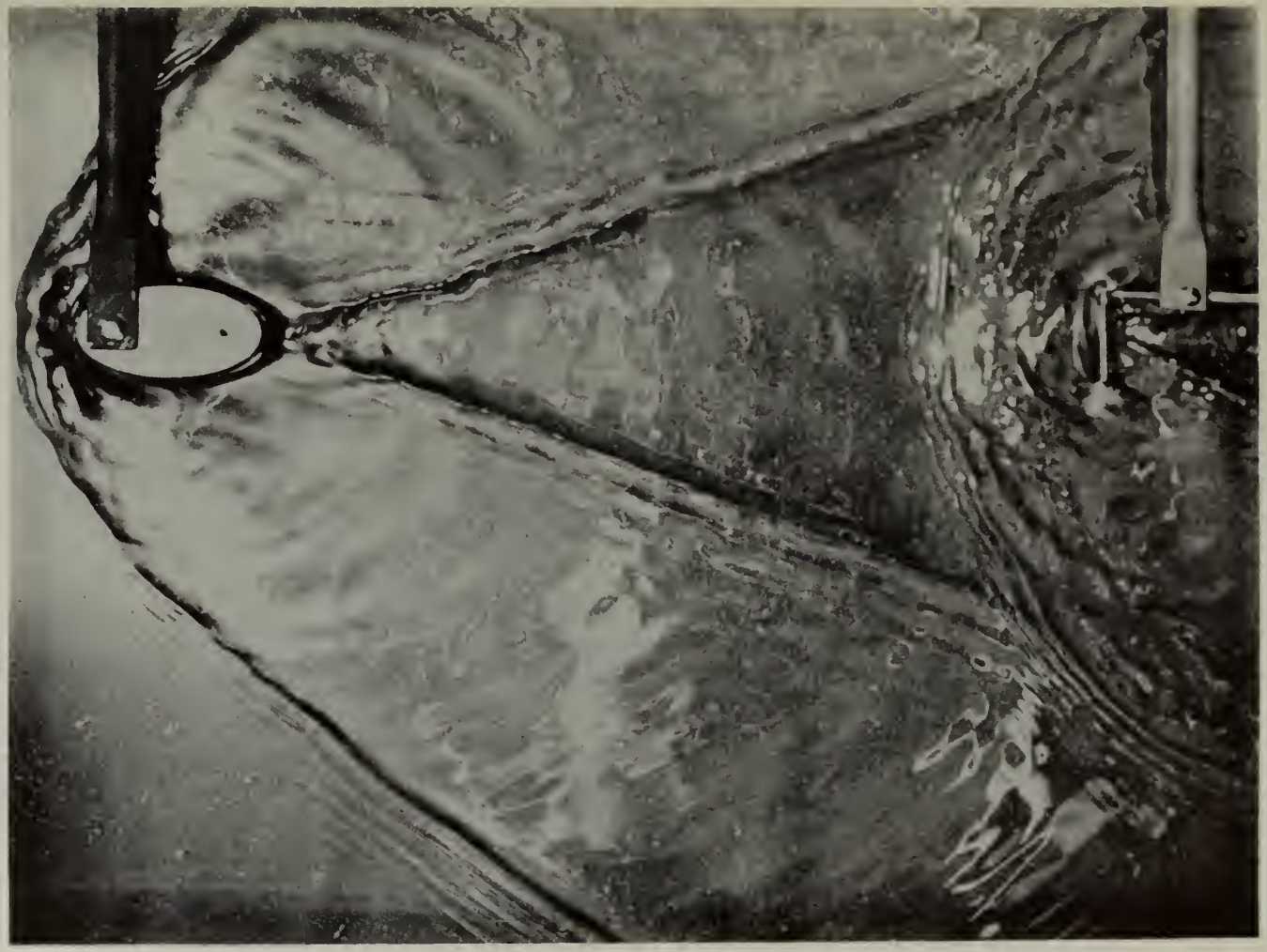

FIG. 24
ELLIPTICAL CYLINDER - FLAT DISK COMBINATION
(9" SEPARATION - M_∞ = 2.03)

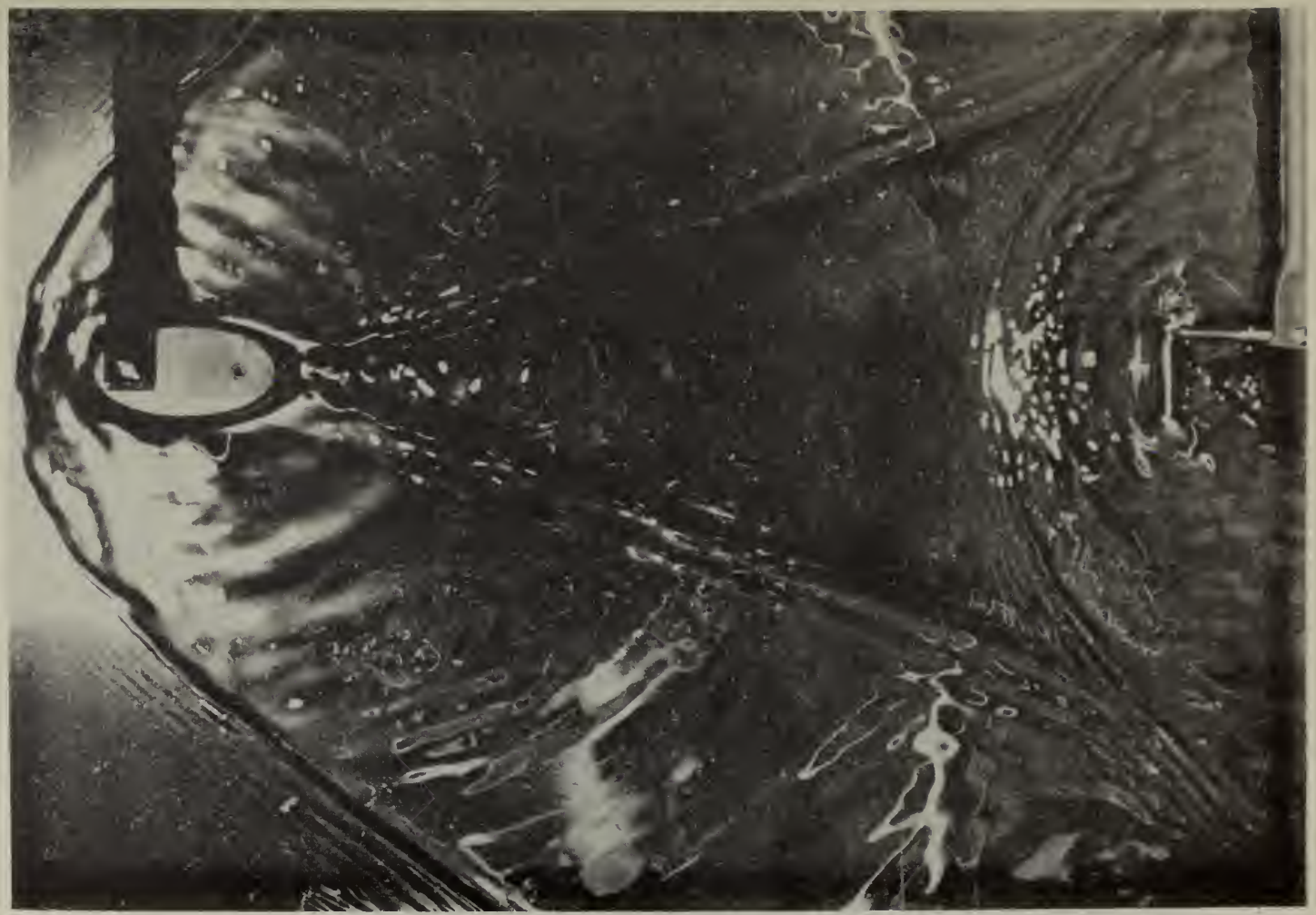

FIG. 25
ELLIPTICAL CYLINDER - FLAT DISK COMBINATION
(10" SEPARATION - M_∞ = 2.02)

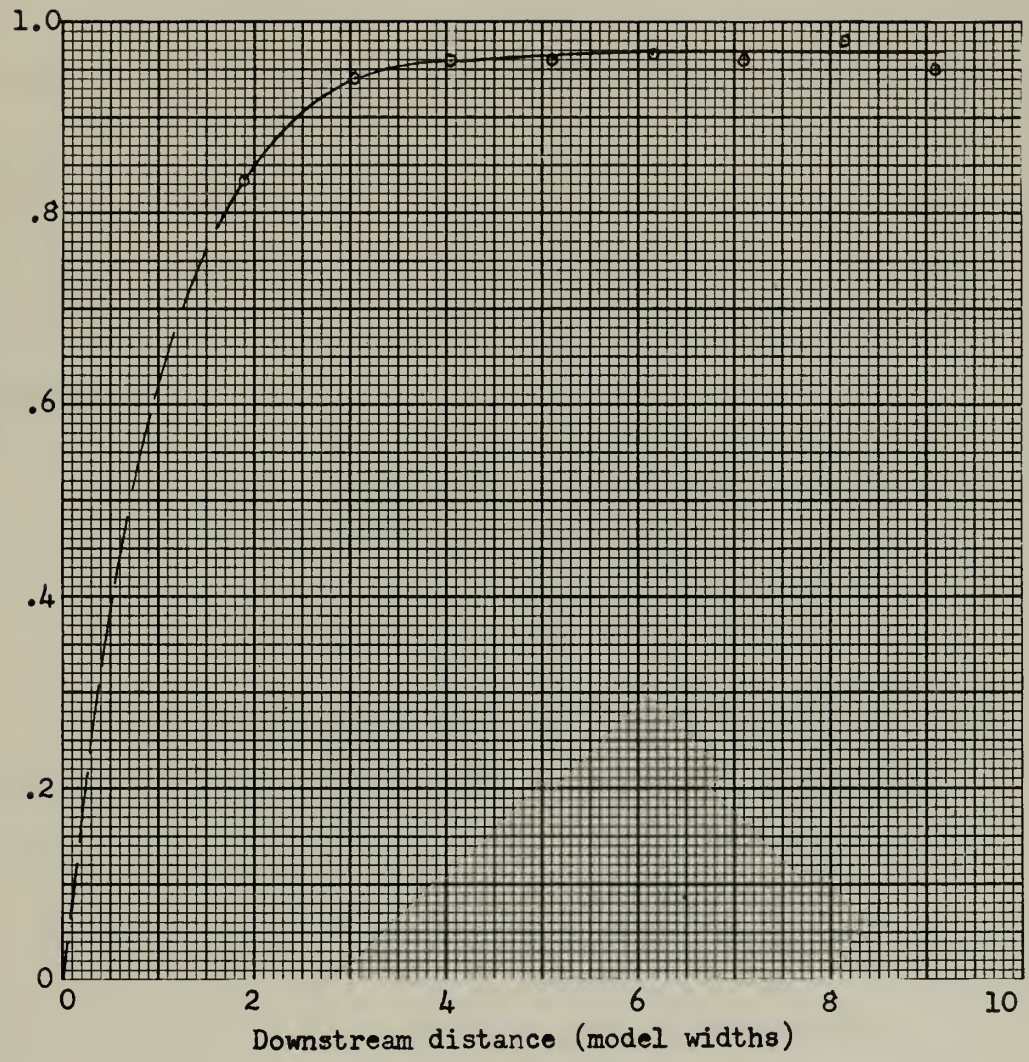

FIG. 26
MACH NUMBER RECOVERY IN THE WAKE
OF AN ELLIPTICAL CYLINDER AT M_∞ = 2.00

APPENDIX A

SUMMARY OF HYDRAULIC ANALOGY THEORY

It has been known for some time that an analogy exists between the flow of a liquid with a free surface and the flow of a compressible gas. Early mathematical treatments of the analogy were made by Jouget and Riabouchinsky. In 1938, Preiswerk[1] made the first really comprehensive theoretical and experimental investigation of this phenomenon. In more recent years, a great deal of interest has been shown by numerous groups in the hydraulic analogy. Especially notable among these groups has been the National Advisory Committee for Aeronautics[5].

The following is a summary of the theory and mathematical development of the hydraulic analogy.

Two assumptions are made in the mathematical development:

a. The flow is irrotational.

b. The vertical accelerations at the free surface of the liquid are negligible compared with the acceleration of gravity. Therefore, the pressure in the liquid at any point depends only on the height of the free surface above that point.

Consider a water channel consisting of a large tank in which the depth of the water, d_o, is constant, and an open duct leading from the tank in which the depth of the water, d, varies with distance from the tank. The floor of the open duct is an extension of the floor of the tank, and is perpendicular to the gravity field of the Earth. If the vertical coordinate, z, is measured from the floor of the channel, the Bernoulli equation is:

$$p + \frac{\rho}{2}V^2 + \rho g z = p_o + \rho g z_o$$

or

$$V^2 = 2g(z_o - z) + \frac{2(p_o - p)}{\rho} \tag{A-1}$$

Utilizing assumption b above:

$$p_o = g(d_o - z_o) \tag{A-2a}$$

and

$$p = g(d - z) \tag{A-2b}$$

Direct substitution into equation (A-1) gives

$$V^2 = 2g(d_o - d) = 2g \Delta d \tag{A-3}$$

Since equation (A-3) does not contain z, the velocity at any point in the open duct is constant over the entire depth and is given only by the difference in depth Δd between the total head and the free level. Δd, at the most, is equal to d_o. Therefore, the maximum attainable velocity is

$$V_{max} = \sqrt{2gd_o} \tag{A-4}$$

The corresponding equations for the velocity of a gas are

$$V^2 = 2g(h_o - h) = 2gc_p(T_o - T) \tag{A-5a}$$

and

$$V_{max} = \sqrt{2gh_o} = \sqrt{2gc_pT_o} \tag{A-5b}$$

Therefore, if the ratio V/Vmax for gas is equated to V/V_{max} for water,

$$\frac{d_o - d}{d_o} = \frac{h_o - h}{h_o} = \frac{T_o - T}{T_o}$$

or

$$\frac{d}{d_o} = \frac{T}{T_o} \tag{A-6}$$

The continuity equation expresses the fact that, for a prizm of space in an incompressible fluid, outgoing volume equals the incoming volume . The equation of continuity for water is

$$\frac{\partial(ud)}{\partial x} + \frac{\partial(vd)}{\partial y} = 0 \qquad \text{(A-7)}$$

The continuity equation for two-dimensional compressible gas flow is

$$\frac{\partial(u\rho)}{\partial x} + \frac{\partial(v\rho)}{\partial y} = 0 \qquad \text{(A-8)}$$

It may be seen that equations (A-7) and (A-8) are of the same form. From these equations we may derive a further condition for the analogy, that the density of gas flow corresponds to the water depth d. Thus,

$$\frac{d}{d_o} = \frac{\rho}{\rho_o} \qquad \text{(A-9)}$$

Previously, however, it was seen that water depth d was the analogous magnitude for the gas temperature T (equation (A-6). This is possible only if a very definite assumption is made regards the nature of the comparison gas. For adiabatic isentropic flow in a gas

$$\frac{\rho}{\rho_o} = \left(\frac{T}{T_o}\right)^{\frac{1}{\gamma-1}}$$

and since, in the analogy, from equations (A-6) and (A-9)

$$\frac{\rho}{\rho_o} = \frac{d}{d_o} = \frac{T}{T_o}$$

then

$$\frac{T}{T_o} = \left(\frac{T}{T_o}\right)^{\frac{1}{\gamma-1}}$$

which is satisfied only if $\gamma = 2.0$.

From the gas relation

$$\frac{p}{p_o} = \left(\frac{\rho}{\rho_o}\right)^{\gamma}$$

it may be seen, since $\gamma = 2.0$, that

$$\frac{p}{p_o} = \left(\frac{d}{d_o}\right)^2 \tag{A-10}$$

The velocity potential for water is given by the equation

$$\phi_{xx}\left(1 - \frac{\phi_x^2}{gd}\right) + \phi_{yy}\left(1 - \frac{\phi_y^2}{gd}\right) - 2\phi_{xy}\,\frac{\phi_x\,\phi_y}{gd} = 0 \tag{A-11}$$

and the corresponding equation for a gas is

$$\phi_{xx}\left(1 - \frac{\phi_x^2}{a^2}\right) + \phi_{yy}\left(1 - \frac{\phi_y^2}{a^2}\right) - 2\phi_{xy}\,\frac{\phi_x\phi_y}{a^2} = 0 \tag{A-12}$$

Therefore, for identical expressions,

$$gd = a^2 \tag{A-13}$$

From equations (A-11) and (A-12), the velocity $\sqrt{gd}$ in the liquid flow is seen to correspond to the velocity of sound in gas flow. It has been shown (5) that $\sqrt{gd}$ is the velocity of propagation of surface waves, the wave lengths of which are large in comparison with the water depth. The ratio of $V/\sqrt{gd}$ in the liquid flow corresponds to the Mach number V/a in the gas flow.

If the velocity of the liquid flow is less than $\sqrt{gd}$ ($M<1$), the water is said to be "streaming". If the velocity of the liquid flow is greater than $\sqrt{gd}$ ($M>1$), the water is said to be "shooting".

In shooting water under certain conditions, the velocity of the flow may strongly decrease for short distances and the depth may increase. An unsteady motion of this type is called a hydraulic jump. Hydraulic jumps of small intensity are propagated with the velocity $\sqrt{gd}$, corresponding to Mach waves in compressible gas flow.

The analogy may be summarized in tabular form as follows:

Significant quantities and characteristics of two-dimensional compressible gas flow, $\gamma = 2.0$	Corresponding values in analogous liquid flow
Temperature ratio, T/T_o	Water-depth ratio, d/d_o
Density ratio, ρ/ρ_o	Water-depth ratio, d/d_o
Pressure ratio, p/p_o	Square of water-depth ratio, $(d/d_o)^2$
Velocity of sound, $a = \sqrt{\frac{\gamma p}{\rho}}$	Wave velocity, $\sqrt{gd}$
Mach number, V/a	Mach number, $V/\sqrt{gd}$
Subsonic flow	Streaming water
Supersonic flow	Shooting water
Shock wave	Hydraulic jump

APPENDIX B

FORM AND LOCATION OF DETACHED SHOCK WAVES AHEAD OF PLANE BODIES

The following is a condensation of pertinent portions of Moeckel's approximate method for predicting form and location of detached shock waves ahead of plane bodies (3). Computations used in predicting the form and location of detached shock waves ahead of models used in this experiment are included in Appendix C.

The representation of flow with detached shock waves used in this analysis is shown in Fig. B-1. The region of subsonic flow is bounded by the portion of the detached wave below its sonic point, S, by the portion of the body contour upstream of its sonic point SB, and by the sonic curve between S and SB. If the form of the detached wave is known, the location of S on the shock can immediately be determined, because for a given M_∞ the angle φ_S for which sonic velocity exists behind the shock is known from shock theory[6]. The flow direction λ_S at this point is then also known. The sonic curve is shown in Fig. B-1 as a straight line. This approximation is used throughout the analysis, although more exact computations, as well as experimental results, indicate that the form may depend considerably on the shape of the nose or leading edge. To the degree of approximation of the present method, however, such variations appear to be unimportant. With the simplified picture shown in Fig. B-1, approximate expressions can be derived for the shock location relative to the body sonic point.

Evidence is available to show that, for bodies with sharp or well-defined shoulders, the sonic point is located at the shoulder.

For more gradually curved bodies, such as ogives or ellipses, the location of the sonic point may be estimated to be at the point where the contour of the body is inclined at the wedge angle corresponding to shock detachment.

The most typical characteristics of detached waves are that: (a) they are normal to the free stream at their foremost point; and (b) they are asymptotic to the free-stream Mach lines at large distances from their foremost point. A simple curve that has these characteristics is an hyperbola represented by

$$\beta y = \sqrt{x^2 - x_0^2} \tag{B-1}$$

where β is the cotangent of the Mach angle and x_0 is the distance from the vertex of the wave to the intersection of its asymptotes. For the purpose of the analysis, the hypothesis is made that to the degree of approximation required, all detached waves in the region between the axis and the sonic point S may be represented by equation (B-1).

With this form of detached wave, the angle between the stream direction and the tangent to the shock at any point is obtained from (Fig. B-1)

$$\frac{dy}{dx} = \tan \varphi = \frac{x}{\beta \sqrt{x^2 - x_0^2}} = \frac{\sqrt{x_0^2 + \beta^2 y^2}}{\beta^2 y} \tag{B-2}$$

The location of S is then

$$y_S = \frac{x_0 \cot \varphi_S}{\beta \sqrt{\beta^2 - \cot^2 \varphi_S}} \tag{B-3}$$

$$x_S = \frac{x_0}{\sqrt{\beta^2 - \cot^2 \varphi_S}} \tag{B-4}$$

If the y-coordinate of the body sonic point is used as the reference dimension, then the form of the shock wave is given by

$$\frac{y}{y_{SB}} = \frac{1}{\beta}\sqrt{\left(\frac{x}{y_{SB}}\right)^2 - \left(\frac{x_0}{y_{SB}}\right)^2} \qquad \text{(B-5)}$$

where, from equation (B-3),

$$\frac{x_0}{y_{SB}} = \beta \frac{y_S}{y_{SB}}\sqrt{\beta^2 \tan^2 \varphi_s - 1} \qquad \text{(B-6)}$$

From the equation (B-4) the dimensionless location of the shock sonic point is

$$\frac{x_S}{y_{SB}} = \frac{\beta \frac{x_0}{y_{SB}}}{\sqrt{\beta^2 - \cot^2 \varphi_s}} \qquad \text{(B-7)}$$

The distance from the foremost point of the shock to the x-coordinate of the body sonic point is

$$\frac{L}{y_{SB}} = \frac{x_{SB}}{y_{SB}} - \frac{x_0}{y_{SB}} \qquad \text{(B-8)}$$

where, from Fig. B-1,

$$\frac{x_{SB}}{y_{SB}} = \frac{x_S}{y_{SB}} + \left(\frac{y_S}{y_{SB}} - 1\right)\tan \eta \qquad \text{(B-9)}$$

If equations (B-6), (B-7) and (B-9) are combined to eliminate all unknown coordinates except y_S and L, equation (B-8) becomes

$$\frac{L}{y_{SB}} = \frac{y_S}{y_{SB}}(C + \tan \eta) - \tan \eta \qquad \text{(B-10)}$$

where

$$C = \beta\left(\beta \tan \varphi_S - \sqrt{\beta^2 \tan^2 \varphi_S - 1}\right) \qquad \text{(B-11)}$$

Inasmuch as β and φ_S are known for any given free-stream Mach number, only quantities y_S/y_{SB} and η remain to be determined to predict the relation between the sonic point on a body and the location of its detached wave.

The continuity equation is applied to the fluid that passes the sonic line to provide

$$\frac{y_S}{y_{SB}} = \left[1 - \frac{(p_o)_\infty}{(p_o)_c}\ \sigma \cos \eta\right]^{-1} \qquad \text{(B-12)}$$

where σ is the contraction ratio required to decelerate the free stream to sonic velocity isentropically.

The appropriate value of η to be used remains to be established. On the basis of the analogy between one-dimensional channel flow and flow with detached shock waves, the sonic line is assumed to be normal to the average flow direction in its vicinity. At S the inclination of the flow is known to be λ_S; whereas at SB the inclination is assumed to be λ_d. If the arithmetic mean of the inclinations at the two extremities is used, the expression for η becomes:

$$\eta = \frac{\gamma}{2} (\lambda_d + \lambda_S) \qquad \text{(B-13)}$$

Because λ_S differs only slightly from λ_d, the inclination of the sonic line for plane flow is assumed to be simply $\eta = \lambda_S$.

Values of y_S/y_{SB} obtained from equation (B-12) are shown as functions of M_∞ in the neighborhood of $M_\infty = 2.00$ in Fig. B-2. The variation of x_0/y_{SB} with M_∞, as computed from equation (B-6), is shown in Fig. B-3. Values of L/y_{SB} obtained from equation (B-10) are shown in Fig. B-4.

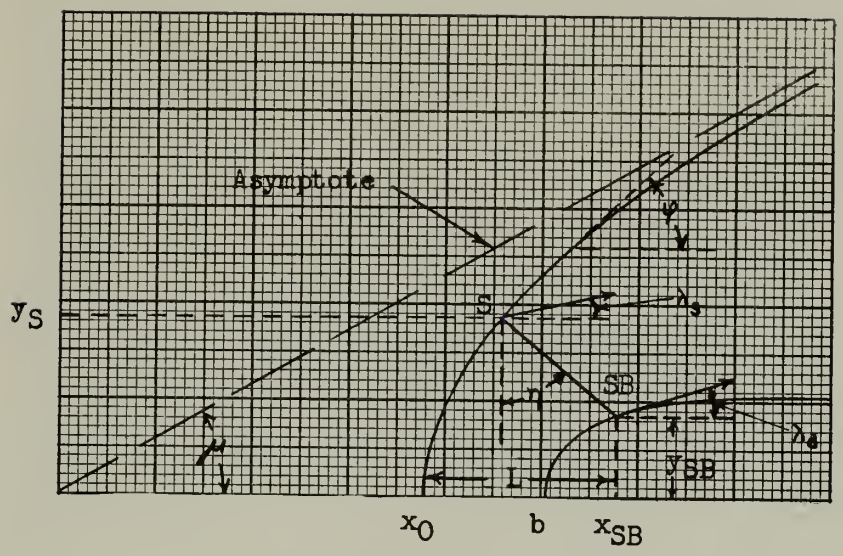

Fig. B-1
Representation of flow with detached shock wave and notation used in analysis

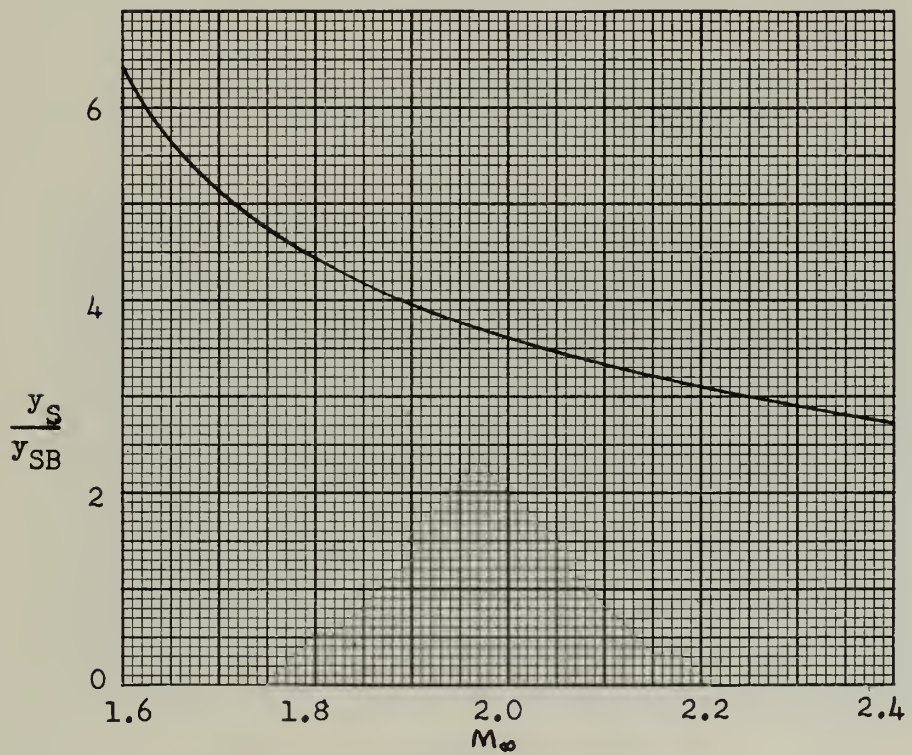

Fig. B-2
Parameter used for determination of shock wave form and location

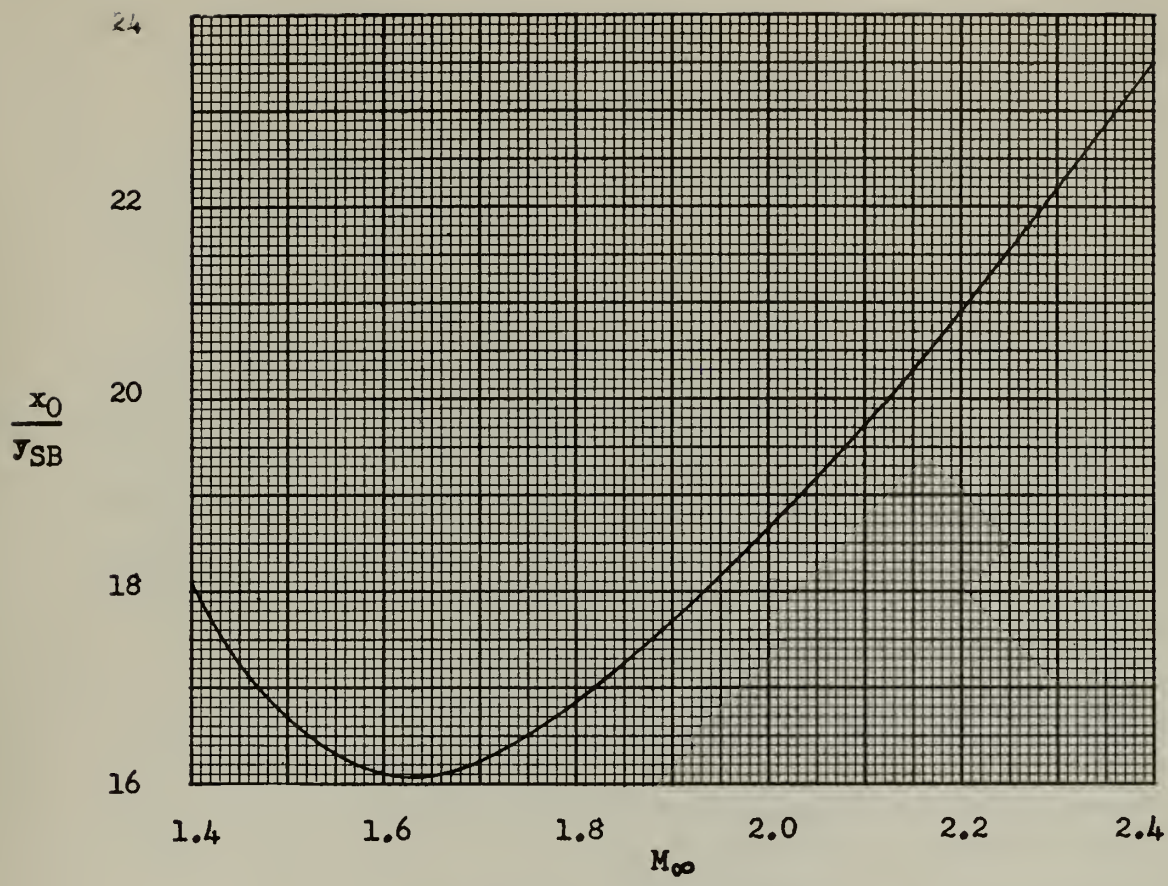

Fig. B-3
Parameter used for determination
of shock wave form and location

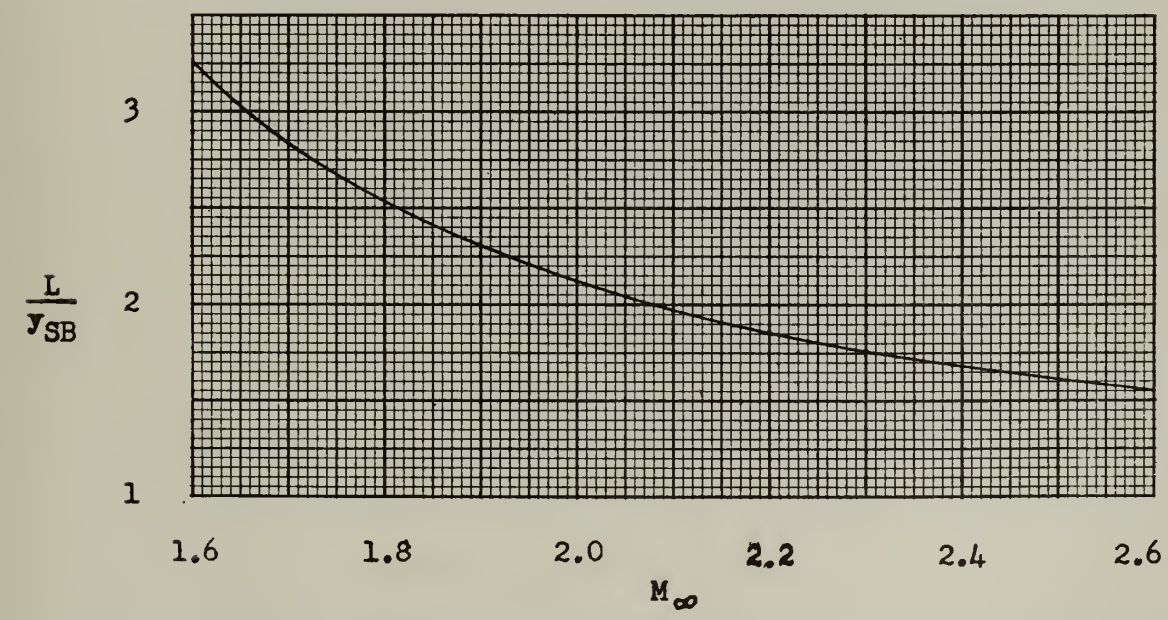

Fig. B-4
Theoretical shock wave location

APPENDIX C

SAMPLE CALCULATIONS

1. Predicted form and location of detached shock waves ahead of models.

It is seen in Appendix B that the reference dimension upon which to base the prediction of the form and location of the detached shock waves ahead of a model is y_{SB}. This dimension for an elliptical model, is dependent upon the shock detachment angle λ_d for a wedge in two-dimensional flow. From Ref. 6

$$\lambda_d = \frac{4}{3\sqrt{3}\,(\gamma + 1)} \quad \frac{(M_\infty{}^2 - 1)^{1.5}}{M_\infty{}^2} \tag{C-1}$$

Substituting the analogous gas constant, $\gamma = 2.00$, and the test Mach number, $M_\infty = 2.00$, into equation (C-1) gives

$$\lambda_d = 0.333 \text{ radians} = 19.1 \text{ degrees}$$

The equation for the cross section of the elliptical model is

$$\frac{x^2}{1} + \frac{y^2}{(\frac{1}{2})^2} = 1 \tag{C-2}$$

By setting the derivative of equation (C-2) equal to tan λ_d, the x-coordinate of the body sonic point, measured from mid-chord, is

$$x = \pm 0.5675 \text{ inch}$$

Substituting this value into equation (C-2) gives

$$y_{SB} = 0.4115 \text{ inch} \tag{C-3}$$

Measured from the leading edge of the model, the x-coordinate of the body sonic point is

$$x = 1 - 0.5675 = 0.4325 \text{ inch}$$

For the flat disk model, the body sonic point is at the shoulder of the model. Thus, for the flat disk model

$$y_{SB} = 0.500 \text{ inch} \qquad (C\text{-}4)$$

From Figs. B-2, B-3 and B-4, the following non-dimensional quantities, for $M_\infty = 2.00$ are found:

$$\frac{L}{y_{SB}} = 2.12$$

$$\frac{y_S}{y_{SB}} = 3.60$$

$$\frac{x_0}{y_{SB}} = 18.65$$

From the foregoing, the following table may be computed:

Quantity	Elliptical Model	Flat Disk Model
L	0.872 inch	1.06 inches
y_S	1.480 inches	1.80 inches
x_0	7.670 inches	9.352 inches
$x_{SB} = x_0 + L$	8.542 inches	10.385 inches

By substituting into equation (B-1), the theoretical shock wave coordinates for the two models are computed and plotted in Figs. C-1 and C-2.

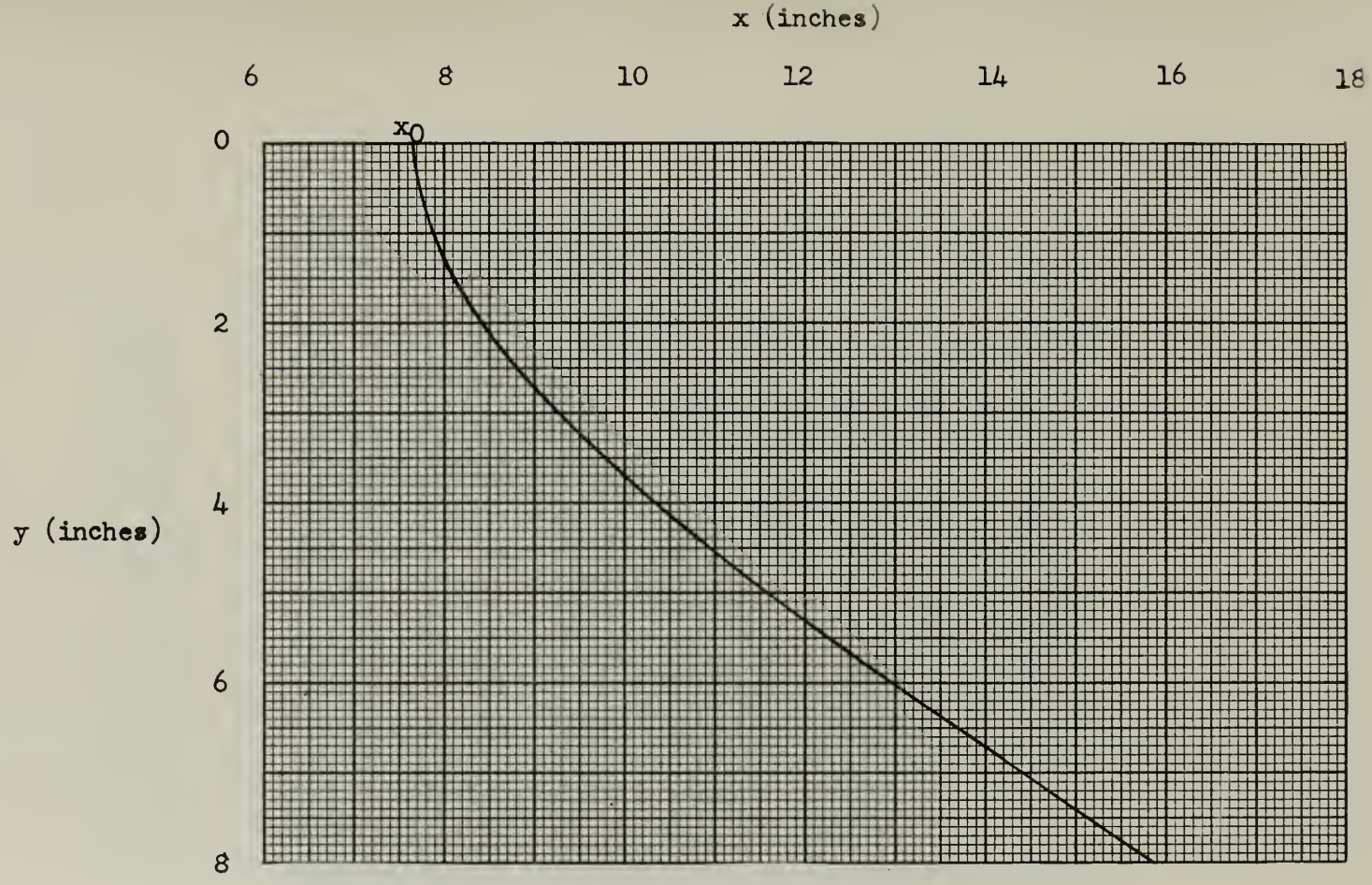

Fig. C-1
Theoretical detached shock wave for
elliptical model at $M_\infty = 2.00$ ($\gamma = 2.00$)

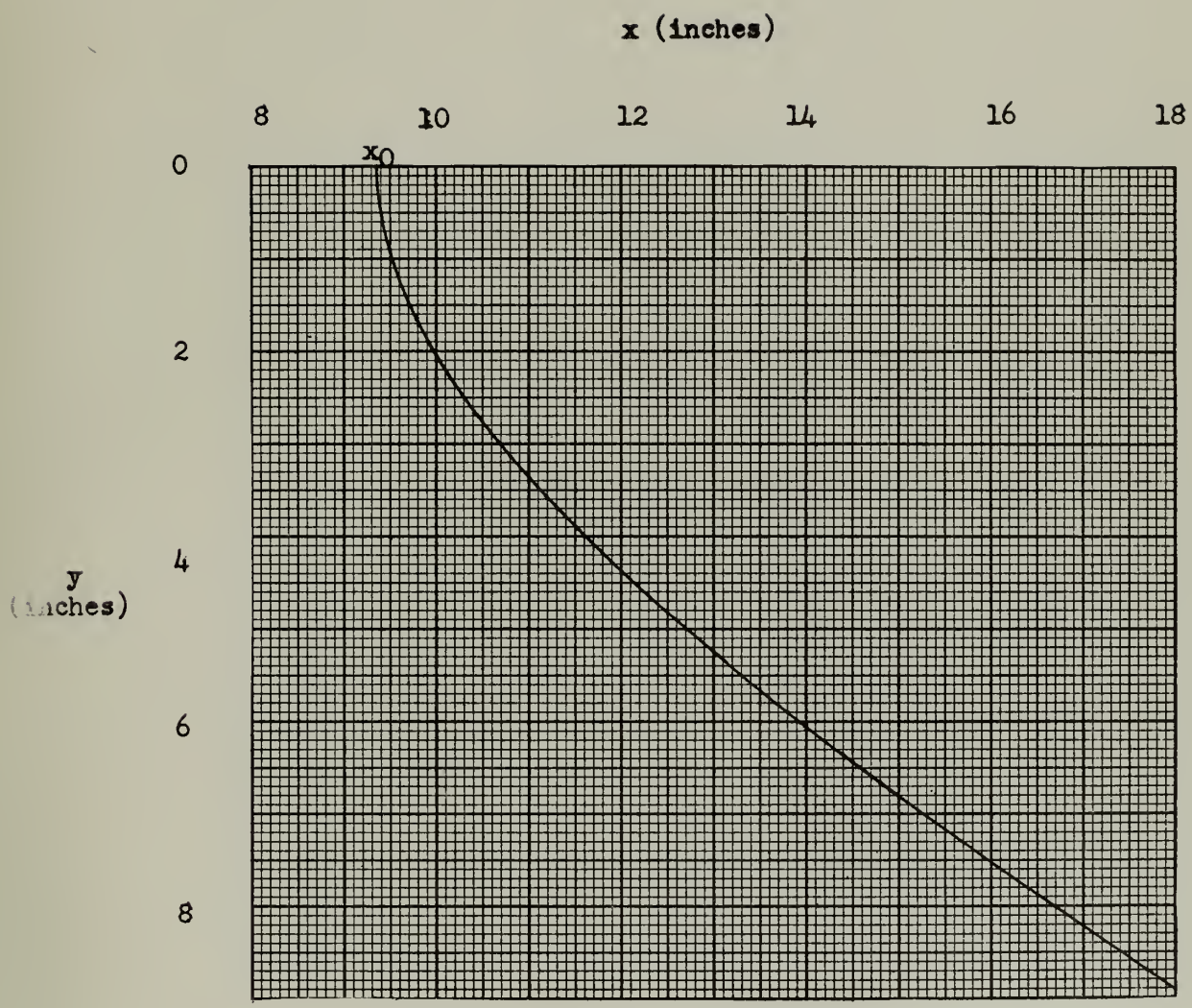

Fig. C-2
Theoretical shock wave for flat disk model in air ($\gamma = 1.4$) at $M_\infty = 2.00$

Thesis
G2577

35766

Geer

A study of the wake at supersonic air flow of an elliptical body ...

Thesis
G2577

35766

Geer

A study of the wake at supersonic air flow of an elliptical body - flat disk combination using hydraulic analogy to compressible air flow.

thesG2577
A study of the wake at supersonic air fl
3 2768 002 02552 0
DUDLEY KNOX LIBRARY